

## Structure-Property Correlation of Sol-Gel Processed $\text{Co}_{0.5}\text{Ti}_{0.5}\text{ZnFeO}_4$ Ceramic

K. Vijaya Kumar<sup>1\*</sup>, M. Lakshmi<sup>2</sup>, M Buchi Suresh<sup>3</sup>

<sup>1</sup>Department of Physics, Jawarharlal Nehru Technological University Hyderabad College of Engineering, Nachupally (Kondagattu), Karimnagar-Dist., 505501, A. P., INDIA.

<sup>2</sup>Department of Physics, SSJ Engineering College, V. N. Pally, Hyderabad, 500075, A.P., INDIA.

<sup>3</sup>Centre for Ceramic Processing, International Advanced Research Centre for Powder Metallurgy and New Materials, Balapur, Hyderabad, 500005, A. P., INDIA.

### Abstract

Titanium doped Cobalt Zinc Ferrite nano powder of chemical composition  $\text{Co}_{0.5}\text{Ti}_{0.5}\text{ZnFeO}_4$  was synthesized using sol-gel method and calcinated at different temperatures ranging from 500-800 °C. The X-ray diffraction (XRD) and Fourier Transform Infrared techniques (FTIR), Scanning Electron Microscopy (SEM) and electrical properties were carried out at room temperature. The grain size becomes larger with increase of calcination temperature ranging from 47.71-83.62 nm. The X-ray diffraction studies reveal the formation of single phase cubic spinel structure. The SEM micrographs show the uniform distribution of the particles, the average size was estimated to be 0.350  $\mu\text{m}$ . IR absorption bands are observed around 600  $\text{cm}^{-1}$  and 400  $\text{cm}^{-1}$  of the tetrahedral and octahedral sites respectively. The effect of calcination temperature on electrical properties was studied and conduction phenomenon in the samples is discussed.

**Keywords:** Ferrites, Sol-gel technique, XRD, SEM, EDS, FTIR, Dielectric constant, Dielectric loss

### I. Introduction

In recent years, ferrite nano-particles have drawn major attention because of their unique physical properties, such as electrical conductivity, optical band gap, refractive index and magnetic properties and superior mechanical properties such as hardness of nanomaterials and chemical properties compared with their counterpart bulk materials. Polycrystalline nano-ferrite particles have become immensely popular magnetic materials for a wide variety of applications such as electronic ignition systems, generators, vending machines, medical implants, wrist watches, inductor core, transformer circuits, magnetic sensors and recording equipment, telecommunications, magnetic fluids, microwave absorbers, other high-frequency applications, etc [1].

Cobalt-zinc ferrite as a special case has interesting properties such as high mechanical hardness, high Curie temperature, low porosity, high chemical stability and reasonable cost [2]. They are also used in radio-frequency circuits, high quality filters, rod antennas, transformer cores, high-speed digital tapes, read/write heads and other devices [3, 4]. A large number of methods have been developed to prepare Co-Zn nano ferrite, such as the co-precipitation, ceramic technique, forced hydrolysis, microwave combustion method, salvo thermal method, the standard solid-state reaction technique, solgel method and the PEG – assisted hydro thermal method. Among them we have selected the sol-gel method [5].

Sol-gel method has the advantage of good stoichiometric control and production of ultrafine

particles with a uniform size distribution in a relatively short processing time. It is a simple process, which saves time and energy consumption over the traditional methods and requires only low sintering temperature [6]. Recent studies have shown that reduction in the size of magnetic materials may lead to novel properties improved better than to the properties of the bulk materials, due to small volume (super paramagnetism) or high surface to volume ratio (spin canting).

The diversity in properties of ferrites has paved the way for the development of a wide variety of ferrites for various applications such as permanent magnets and electrical and electronic compounds [7, 8]. Their properties are very sensitive to the type of substitution and sintering conditions such as temperature, time and heating rate [9]. A selective magnetic dilution is very important in ferrites. The nonmagnetic ions that can be used in such dilution should have ionic radius comparable with that of the magnetic ions. In this case we can improve the electronic and magnetic properties of ferrite samples. It is found that small substitution of Fe ions by rare earth ion may favorably influence the magnetic and electrical properties of ferrite. It is thus possible to obtain a good magnetic material for use in high frequency applications.

The interesting and useful magnetic and electrical properties of soft ferrites are governed by the choice of the cations along with  $\text{Fe}^{2+}$ ,  $\text{Fe}^{3+}$  ions and their distribution between tetrahedral (A) and octahedral (B) sites of the spinel ferrite, as well as

preparation conditions [10]. Although a tremendous work has been reported on Zn doped Cobalt ferrites, but the simultaneously huge investigation is required on the variation of electrical and magnetic properties of Co-Zn nano ferrites with  $Ti^{4+}$  ions [11-13]. In the present work, sol-gel method is used to prepare  $Co_{0.5}Ti_{0.5}ZnFeO_4$  nano powder. Further the effect of the annealing temperature on the structural, micro structural and electrical properties of  $Co_{0.5}Ti_{0.5}ZnFeO_4$  was investigated. In the present work, systematic study of the electrical impedance spectroscopy, X-ray density, SEM, bulk density and porosity of cobalt zinc ferrites have been carried out in order to find the relationship of these properties with the annealing temperature.

## II. Experimental Procedure:

$Fe(NO_3)_3 \cdot 9H_2O$  (99.0% pure LOBAL Chemie),  $Zn(NO_3)_2 \cdot 6H_2O$  (99.0% pure SDFCL),  $Co(NO_3)_2 \cdot 6H_2O$  (99.0% pure SDFCL),  $TiCl_4$  (99.0% pure SDFCL) and  $C_6H_8O_7 \cdot H_2O$  (Hydrated citric acid)(99.5% pure MERK) were used as raw materials. Stoichiometric amount of metal nitrates and appropriate dosage of citric acid are dissolved in minimum quantity of deionised water and stirred well. Citric acid helps the homogenous distribution of the metal ions to get segregate from the solutions. After adjusting the metal nitrate and citric acid ratio to 1:1, the mixed solution was neutralized to a pH value of 7 by adding liquid ammonia, since the base catalysts are employed in order to speed up the reaction. After the mixed solution was heated at 60°C on a hot plate and continuously stirred using a magnetic stirrer for 1 hr, the solution turned into brown sol. Then heated at 100°C and stirred constantly, the sol became sticky gel. Increasing the temperature up to 200°C led to the self-ignition of the gel. The dried gel burnt in a self-propagating combustion reaction until all the gel was completely burnt out to form a voluminous and fluffy powder with a large surface area. This powder is further crushed in agate mortar to obtain the nano sized powder. The resultant powder is heated at 500°C, 600°C, 700°C and 800°C, respectively for 4 h to form spinel  $CoZnTi$  Ferrite nano particles. The maximum particle size after grinding was 83.62nm. These powders were pressed into pellets. The diameter and thickness of the pellets are 10 mm and 2 mm, respectively. The pellets were calcinated for 4 h at 950°C.

The X-ray diffraction (XRD) patterns of all the prepared samples were taken by X-ray diffractometer using  $Cu K\alpha$  radiation ( $\lambda=1.54\text{\AA}$ ). The diffraction peaks are broad because of the nano meter size of the crystallite. A careful analysis of the XRD patterns helps to determine the respective planes and face centered cubic structure of these ferrites. Well resolved peaks in XRD pattern clearly indicate the single phase and polycrystalline nature of the samples. The size of crystal is evaluated by measuring the full width half maximum (FWHM) of the most intense

peak (311) from XRD and by using the Debye Scherrer's formula.

The size of the **crystallite** is evaluated using the formula,  $D = 0.94\lambda / \beta \cos\theta$ , where  $D$  is the crystallite size,  $\lambda$  is the wavelength of incident X-ray,  $\theta$  is the diffraction angle and  $\beta$  is the full-width at half maximum (FWHM). For electrical characterization, powders were compacted and sintered at 950°C for 4 h. The AC impedance spectroscopy measurements using two probe method were carried out with solartron SI1260 impedance analyzer. For the electrical measurements ohmic contacts were made by using silver paste on two faces of the samples. For temperature measurements specimens were placed in a furnace where temperature could be controlled.

## III. Results and discussion:-

The XRD patterns of Ti doped cobalt zinc ferrite nano-particles at different calcinations temperatures of 500, 600, 700 and 800°C for 4 h are shown in Fig. 1. Samples show the reflection planes of (111), (220), (311), (222), (400), (422), (511) and (440) which confirm the presence of single-phase of ferrite phase with a face centered cubic structure. Except for the impure phase of  $\alpha-Fe_2O_3$  which is found in all calcined samples and occurs naturally as hematite [14]. The XRD patterns also indicated increase in crystallinity by increasing the calcination temperature, due to the removal of stresses with the heating process.

**Table 1: Variation of particle size, crystallite size, lattice constant and X-ray density with calcination temperature.**

SAMP LE	Calcination Temperature (°C)	Crystallite size (D) nm	LATTICE CONSTANT a(A°)	X-RAY DENSITY g/cc
R5	500	47.71	8.384	5.3702
R6	600	65.13	8.390	5.358
R7	700	83.38	8.392	5.354
R8	800	83.62	8.393	5.353

The values of particle size, lattice parameters and X-ray density are furnished in Table-1. These values are slightly lower than the lattice parameter of the standard pattern (JCPDS 35-1373). From the table-1, it can be clearly understood that with the increase of the calcination temperature, the diffraction peaks become sharper and increase in intensity. This indicates intensification in crystallinity that originates from the increment of crystalline volume ratio due to particle size enlargement of the nuclei [15].

Fig. 2 shows the FTIR spectra of  $Ti_{0.5}Co_{0.5}Zn_{1.0}Fe_{1.0}O_4$  nano particles of all the considered samples in the range of 400 to 4000 $cm^{-1}$ . For ferrites, generally two assigned absorption bands

appear around  $600\text{cm}^{-1}$ , which is attributed to stretching vibration of tetrahedral group Fe-O and that around  $400\text{cm}^{-1}$ , which is attributed to the octahedral group complex Fe-O. The powders heat treated at different temperatures show characteristic absorptions of the ferrite phase with a strong absorption around  $600\text{cm}^{-1}$  and another absorption in the range of  $410\text{-}450\text{cm}^{-1}$ . The difference in the band positions with calcination temperature is expected because of the difference in the  $\text{M}^{2+}\text{-O}^{2-}$  distance for the octahedral and tetrahedral groups. Waldron studied the vibrational spectra of ferrites and attributed the sharp absorption band around  $600\text{ cm}^{-1}$  to the intrinsic vibrations of the tetrahedral groups, and the other band to that of the octahedral groups [16].

Fig. 3 shows the SEM images of  $\text{Co}_{0.5}\text{Ti}_{0.5}\text{ZnFeO}_4$  ferrite prepared by sol-gel process with different calcination temperatures. It can be seen that the grain size becomes larger with the increase of calcination temperature with the size range of 47.71 - 83.62 nm. The increase in grain size results in a decrease of fraction of low coordinated atoms at the surface skin of grains, which decreases the lattice stresses due to inward shrinking atoms lying on the surface. Therefore, the lattice parameter of the prepared samples increased with an increase in grain size. It is obvious that when cell volume increases, the theoretical density decreases. Fig. 4 shows EDS analysis of all the samples and it shows the presence of elements such as Titanium, Cobalt, Zinc and Iron in all the samples.

The particle size distributions of Ti doped Co-Zn ferrite samples are shown in Fig. 5. The results indicate that the samples prepared by the thermal treatment method are uniform in morphology and particle size distribution. The particle sizes increased with increasing calcination temperature (Table 1). The smallest particle size obtained in this study was 7 nm for R5 and particle size reached to 47 nm at the highest calcination temperature for R8. This suggests that several neighboring particles fuse together to increase particle sizes by melting their surfaces [17]. This grain growth of particle size enlargement at higher calcination temperatures has been observed previously in cobalt ferrite [18] and in zinc ferrite [19] systems.

Fig. 6 shows the variation of the dielectric constant with frequency measured at room temperature. In all the samples the dielectric constant decreases with increase in frequency exhibiting a normal ferrimagnetic behaviour. A more dielectric dispersion is observed at lower frequency region and it remain almost independent of applied external field at high frequency side. The sample R5 showed a maximum dispersion while that R8 showed a least frequency dependence. The dielectric dispersion observed in the lower frequency region is due to Maxwell-Wagner interfacial type of polarization, which is in agreement with Koops phenomenological theory [20]. The presence of  $\text{Fe}^{2+}$  ions in excess

amount favours the polarization effects. The decrease in dielectric constant with increase in frequency is due to lag of hopping frequency of electrons between  $\text{Fe}^{2+}$  and  $\text{Fe}^{3+}$  ions against the frequency of external applied ac field and becomes independent beyond a certain limit. The plot of dielectric loss tangent ( $\tan\delta$ ) against log frequency is shown in Fig. 7. All the samples show an increase in  $\tan\delta$  with frequency up to a certain value and decreases with increasing frequency indicating a maximum at about 100 kHz of applied frequencies. Similar types of maxima in the plot of loss tangent versus frequency have been reported for doped Zn ferrite [21] and doped Ti ferrite [22] ferrite systems. The R5 sample however, shows more dielectric loss at low frequency region as compared to other samples, which may be due to the presence of space charge polarization resulting into the more inhomogeneous dielectric structure [23]. The condition for observing a maximum in the dielectric loss of a material is given by the relation  $\omega\tau=1$ , where  $\omega=2\pi f_{\text{max}}$  and  $\tau$  is the relaxation time. Therefore, a maximum can be observed when the jumping or hopping frequency of electrons between  $\text{Fe}^{2+}$  and  $\text{Fe}^{3+}$  becomes nearly equal to the frequency of the applied field [24]. The sharp peak can be observed when both the frequencies exactly matches with each other.

To elicit more information about the mechanism of electrical transport in this compound, impedance measurements are carried out as a function of frequency between 0.1 Hz and 10 MHz. The impedance spectroscopy helps in the separation of grain and grain boundary effects because each of them has different relaxation times, resulting in separate semi-circles in complex impedance plot. The relaxation time ( $\tau$ ) is a parameter that depends on the intrinsic properties of the material governing the distribution of resistive and capacitive components in the material. So, the results obtained using impedance analyser are basically unambiguous and provide true picture of the sample electrical behaviour.

Fig. 8 shows the variation of  $Z''$  with frequency at different temperatures. The plots show that  $Z''$  values attain a peak ( $Z''_{\text{max}}$ ) for all the samples, which shifts to higher frequency with increasing temperature and all the curves merge at higher frequencies. The shifting of peaks towards higher frequency indicates that the relaxation time is decreasing with the increase of temperature. The peak broadening with increasing temperature suggests the presence of temperature dependent electrical relaxation phenomenon in the material [25] and is due to the material in-homogeneity of the polycrystalline sample. The relaxation process is due to the presence of space charges whose mobility increases at higher temperature. This shift in frequency maxima indicates active conduction through the grain boundary. The magnitude of  $Z''_{\text{max}}$  also decreases with increase in temperature. The merger of  $Z''$  values in the high frequency domain may be possibly an indication of the

accumulation of space charges in the material at low frequency and at higher temperature.

Fig. 9 shows the plot of  $Z'$  vs  $Z''$  (Cole-Cole plots) taken over a frequency range of 1 Hz–10MHz of Ti doped cobalt zinc ferrite calcined at different temperatures. It is observed that for R5-R7 samples single deviated semicircular arc is observed and two semicircular arcs could be traced for R8 sample with different values of resistance for grain ( $R_g$ ) and grain boundary ( $R_{gb}$ ). The high frequency semicircle corresponds to a bulk contribution and low frequency corresponds to grain boundary effect. Hence grain and grain boundary effects could be separated at these temperatures. The values of  $R_g$  and  $R_{gb}$  are obtained from the intercepts of the traced semicircles with  $Z'$  axis. It can be clearly noticed that the values of  $R_g$  and  $R_{gb}$  decreases with rise in calcination temperature. Two semicircle arcs of the impedance spectrum can be expressed by an equivalent circuit consisting of a parallel combination of low resistances and constant phase elements connected in series. The spectrum reveals relatively large grain boundary contribution to the total resistivity because close to the grain boundaries, transport properties of the materials are controlled by imperfections, expected to be present in higher concentration than in grains leading to an additional contribution to the grain boundary impedance. The internal space charge created at the grain boundaries may lead to a significant increase in the concentration of mobile effects. The peak frequency for grain boundaries is much smaller than that for grains due to their large resistance and capacitance compared to those of grains.

The AC resistivity was calculated using the formula  $\rho = R \times (t/A)$ , where  $R$  is resistance. It is observed that the AC resistivity decreases with increase in calcinations temperature. Also the resistivity of all the samples was found to decrease with the increase in frequency upto 10MHz. The conduction in ferrites is electronic in nature as proposed by Verway [26]. The charge transfer takes place owing to hopping of electrons between  $Fe^{2+}$  and  $Fe^{3+}$  states at the octahedral sites of the spinel lattice. A variation in electrical resistivity with temperature of heat treatments in  $Co_xFe_{3-y}Zn_xO_4$  system, has been observed by Na et al. [27]. From the above results, it is concluded that the decrease in electrical resistivity was attributed to the increase in electron concentration.

#### IV. Conclusions

Co-Ti-Zn Ferrite with particle size of 7-47 nm were synthesized by sol-gel process and calcined at different temperatures. Different particle size of  $Co_{0.5}Ti_{0.5}ZnFeO_4$  ferrite powders were obtained by varying the calcination temperature and the grain size becomes larger with the increasing calcination temperature. To stabilize the particles, they were thermally treated at various temperatures from 623 to 823 K at which calcination occurred, thereby stabilizing the particles, controlling the growth of the

nano-particles, preventing their agglomeration, and creating a uniform distribution of particle sizes. Particle sizes of 7–47 nm were obtained with calcination temperatures between 623 and 823 K, as confirmed by XRD and SEM analyses.

#### References

- [1] P M Prithviraj Swamy, S Basavarajal, Arunkumar Lagashetty<sup>2</sup>, N V Srinivas Rao<sup>3</sup>, R Nijagunappa<sup>4</sup> And A Venkataraman, Synthesis and characterization of zinc ferrite nanoparticles obtained by self- propagating low- temperature combustion method, Bull. Mater. Sci., Vol. 34, No.7, Dec.2011, pp. 1325-1330.
- [2] Vaidyanathan G, Sendhilnatha S., Characterization of  $Co_{1-x}Zn_xFe_2O_4$  nanoparticles synthesized by co-precipitation method, Physica B 2008; 403: 2157-2167
- [3] A.Hassadee, T.Jutarosaga, W.Onreabroy, Effect of zinc substitution on structural and magnetic properties of cobalt ferrite, Procedia Engineering, 2012; 32: 597-602
- [4] Köseoglu Y, Baykal A, Gözuak F., Structural and magnetic properties of  $Co_xZn_{1-x}Fe_2O_4$  nanocrystals synthesized by microwave method, Polyhedron 2009; 28: 2887-2892.
- [5] Rani, Ritu, Sharma, S. K, Pirota, K. R, Knobel, M, Thakur, Sangeeta, Singh. M, Effect of Zinc concentration on the magnetic properties of Cobalt-Zinc nanoferrite, Ceramics International, 38 (2012) 2389-2394.
- [6] Dong Limin, Han Zhidong, Zhang Yaoming, Wu Ze, Zhang Xianyou, Preparation and sinterability of Mn-Zn Ferrite powders by Sol-Gel method, J. Rareearths, Vol.24. Dec.2006, p.54
- [7] A. Meenakshisundaram, N. Gunasekaran and V.Srinivasan, Distribution of Metal Ions in Transition Metal Manganites  $AMn_2O_4$  (A: Co, Ni, Cu, or Zn), Phys. Status. Solidi (a) 1982: 69 : k15.
- [8] B.V. Bhise, A.K. Ghatage, B.M. Kulkarni, S.D. Lotke and S.A. Patil, Conduction in Mn substituted Ni-Zn ferrites, Bull.Mater.Sci 1996;19 (3): 527.
- [9] M.M. El Sayed, Rare-earth substitution effect on the quality of Mg-Ti ferrite, Ceramics International 33 (2007) 413-418.
- [10] Gul, I.H., Maqsood, A., Structural, magnetic and Electrical properties of Cobalt ferrites prepared by sol-gel route., Journal of Alloys and Compounds, 465 (2008) 227-231.
- [11] Sonal Singhal, Rimi Sharma, Tsering Namgyal, Sheenu Jauhar, Santosh Bhukal, Japinder Kaur, Structural, Electrical and magnetic properties of  $Co_{0.5}Zn_{0.5}Al_xFe_{2-x}O_4$  ( $x=0, 0.2, 0.4, 0.6, 0.8$  and  $1.0$ ) prepared via sol-gel route., Ceramics International, 38 (2012) 2773-2778

- [12] Ana Maria Rangel de Figueiredo Teixeiraa, Tsuneharu Ogasawarab, Maria Cecília de Souza Nóbregab, Investigation of Sintered Cobalt-zinc Ferrite Synthesized by Coprecipitation at Different Temperatures: A Relation between Microstructure and Hysteresis Curves, *Materials Research*, Vol. 9, No. 3, 257-262, 2006
- [13] K.Muthuraman, Synthesis of Nano sized Ce-Co Doped Zinc Ferrite and their Permittivity and Hysteresis Studies, *International Journal of Computer Applications* (0975 – 8887) Volume 32– No.3, October 2011
- [14] P. Laokul, V. Amornkitbamrung, S. Seraphin, S. Maensiri, Characterization and magnetic properties of nanocrystalline  $\text{CuFe}_2\text{O}_4$ ,  $\text{NiFe}_2\text{O}_4$ ,  $\text{ZnFe}_2\text{O}_4$  powders prepared by the Aloe vera extract solution, *Curr. Appl. Phys.* 11 (2011) 101–108
- [15] Y.P. Sui, X.F. Huang, Z.Y. Ma, W. Li, F. Qiao, K. Chen, K.J. Chen, The effect of thermal annealing on crystallization in a-Si:H/SiO<sub>2</sub> multilayers by using layer by layer plasma oxidation, *J. Phys. Condens. Matter.* 15 (2003) 5793–5800
- [16] R.D. Waldron, *Phys. Rev.* 99 (1955) 1727
- [17] K. Maaz, S. Karim, A. Mumtaz, S.K. Hasanain, J. Liu, J.L. Duan, Synthesis and magnetic characterization of nickel ferrite nanoparticles prepared by coprecipitation route, *J. Magn. Mater.* 321 (2009) 1838–1842
- [18] K. Maaz, A. Mumtaz, S.K. Hasanain, A. Ceylan, Synthesis and magnetic properties of cobalt ferrite ( $\text{CoFe}_2\text{O}_4$ ) nanoparticles prepared by wet chemical route, *J. Magn. Mater.* 308 (2007) 289–295
- [19] M.K. S Roy, B. Halder, H.C. Verma, Characteristic length scales of nanosize zinc ferrite, *Nanotechnol.* 17 (2006) 232–237
- [20] C.G. Koops, *Phys. Rev.*, USA 83 (1951) 121
- [21] Batoor, Khalid Mujasam; Kumar, Shalendra; Lee, Chan Gyu; Alimuddin, Study of dielectric and ac impedance properties of Ti doped Mn ferrites, *Current Applied Physics* 9(2009) 1397 – 1406.
- [22] M.B. Reddy, P.V. Reddy, Low-frequency dielectric behaviour of mixed Li-Ti ferrites, *J. Phys. D: Appl. Phys.* 24 (1991) 975
- [23] R.S. Patil, S.V. Kakatkar, P.K. Maskar, S.A. Patil, S.R. Sawant, Dielectric behaviour of  $\text{Li}_{0.5}\text{Zn}_x\text{Zr}_x\text{Fe}_{2.5-2x}\text{O}_4$  ferrites, *Ind. J. Pure & Appl. Phys.* 29 (1991) 589
- [24] L.I. Rabinkin, L.I. Novikova, *Ferrites (Minsk)* (1960) 146
- [25] J. R. Macdonald, *Impedance Spectroscopy Emphasizing solid materials and systems*, John Wiley & Sons, New York, 1987, pp. 191-237
- [26] E.J. Verway, P.W. Hayman and F.C. Romeign, Physical Properties and Cation Arrangement of Oxides with Spinel Structures II. Electronic Conductivity , *J. Chem. Phys.*, 15 (4) (1947)
- [27] J.G. Na, T.D. Lee and S.J. Park, *IEEE Trans. Magn.*, Effects of cation distribution on the magnetic and electrical-properties of cobalt ferrite, 28 (5) (1992) 2433–2435

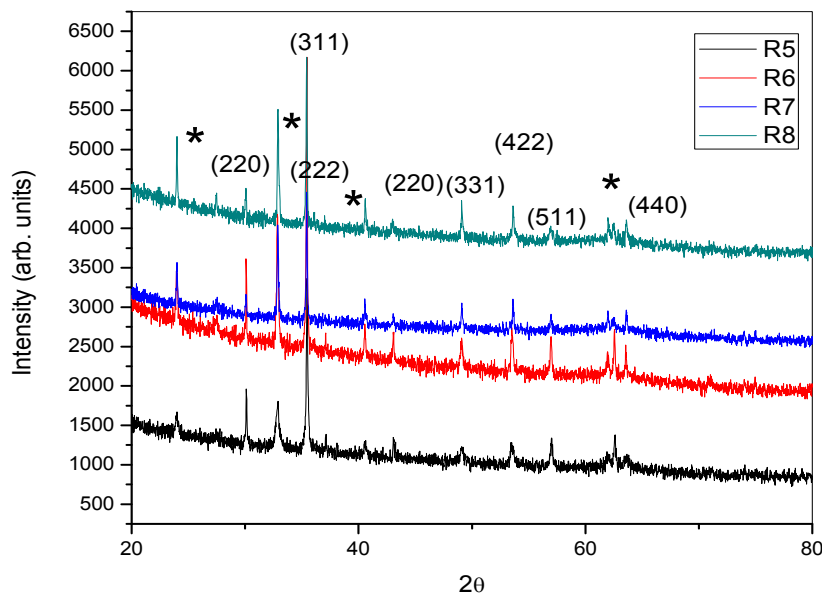


Fig.1: X-ray diffraction patterns of  $\text{Co}_{0.5}\text{Ti}_{0.5}\text{ZnFeO}_4$  powders calcinated at in the temperature range 500-800 °C

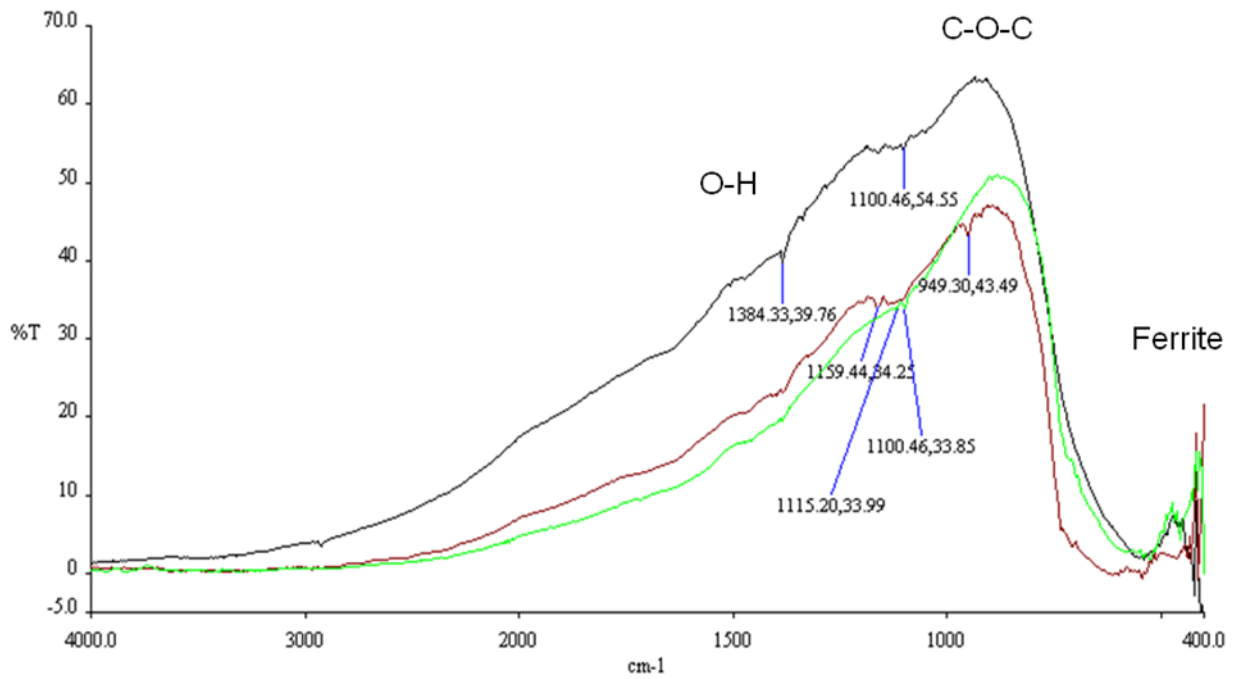


Fig.2: FTIR plots of  $\text{Co}_{0.5}\text{Ti}_{0.5}\text{ZnFeO}_4$  powders calcinated at in the temperature range 500-700 °C

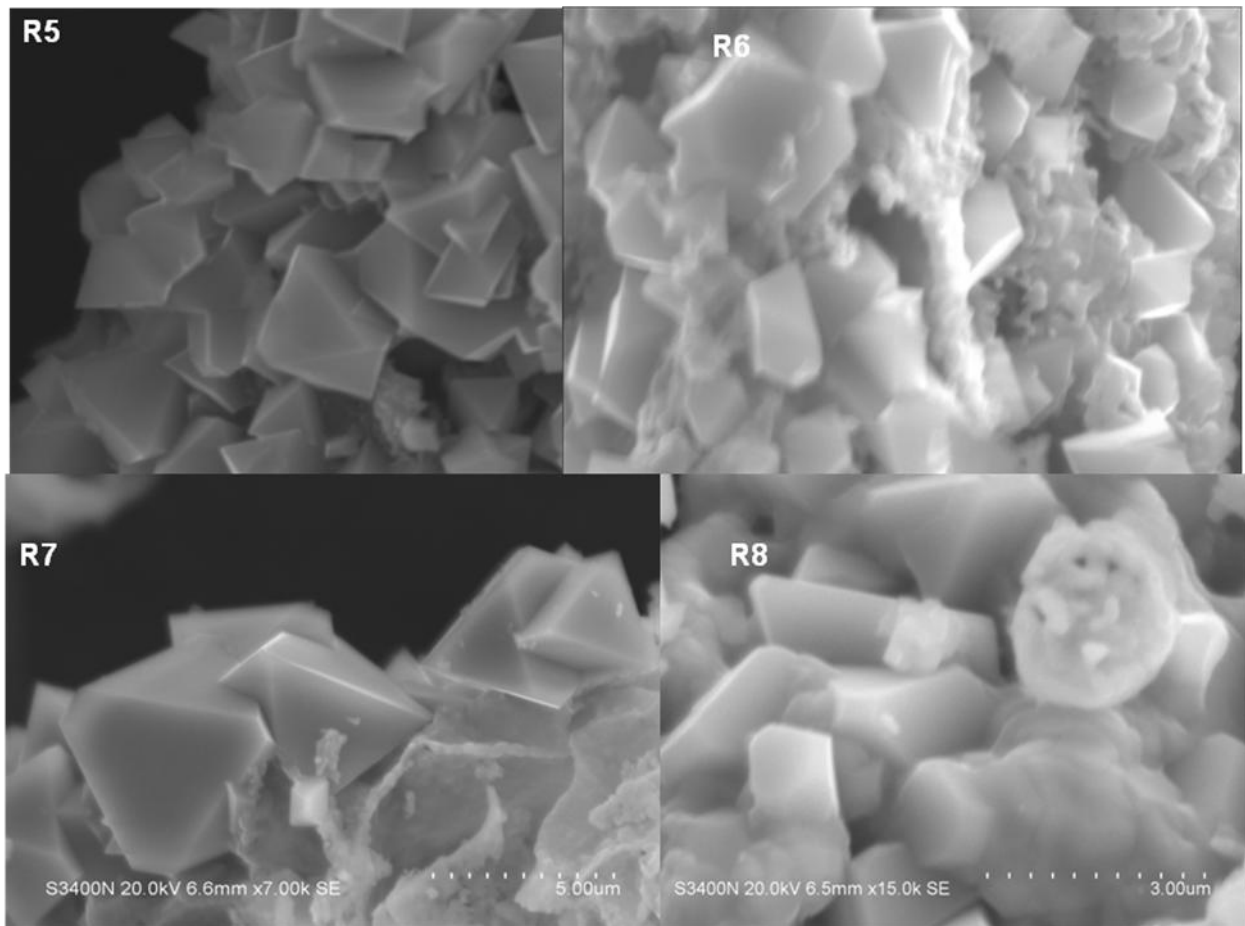


Fig.3: SEM images of  $\text{Co}_{0.5}\text{Ti}_{0.5}\text{ZnFeO}_4$  powders calcinated at in the temperature range 500-800 °C

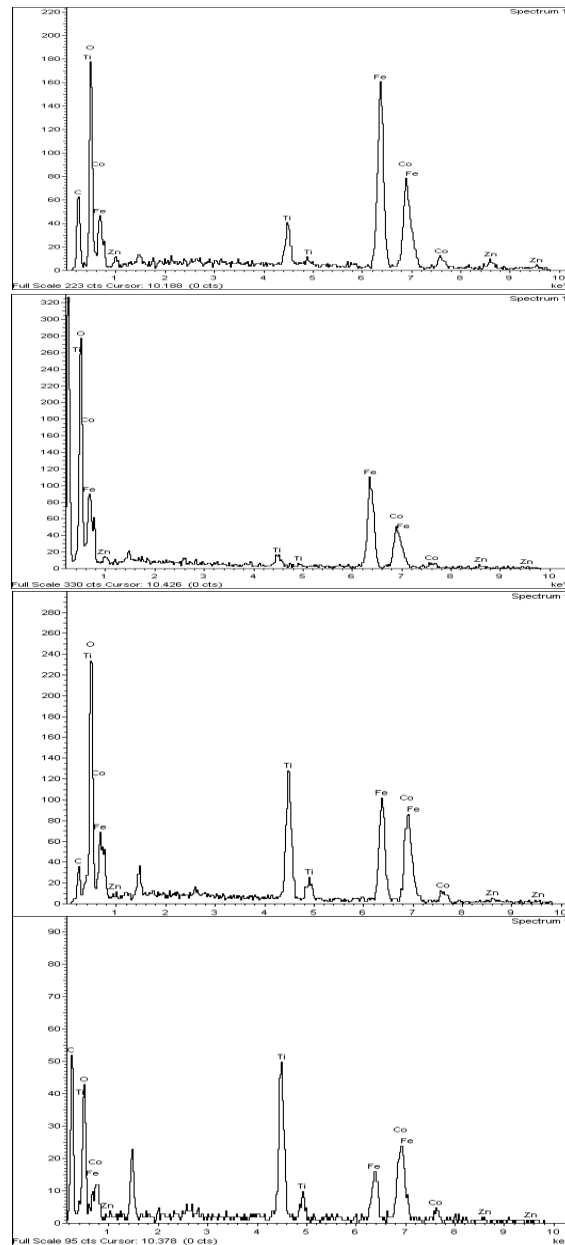


Fig.4: EDS analysis of  $\text{Co}_{0.5}\text{Ti}_{0.5}\text{ZnFeO}_4$  powders calcinated at in the temperature range 500, 600, 700 & 800 °C (top to bottom)

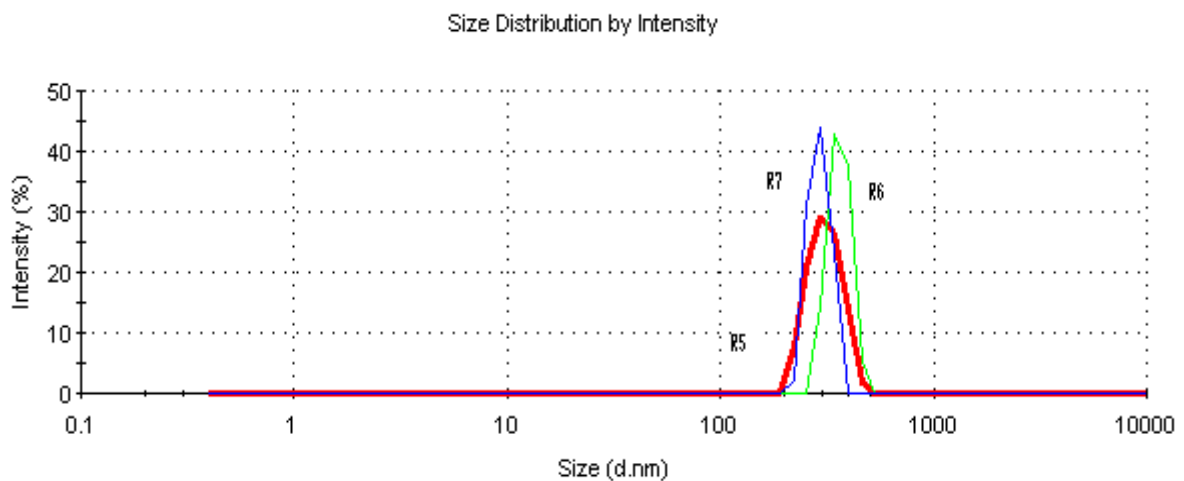


Fig.5: Particle size distribution of the powders heat treated at different temperatures

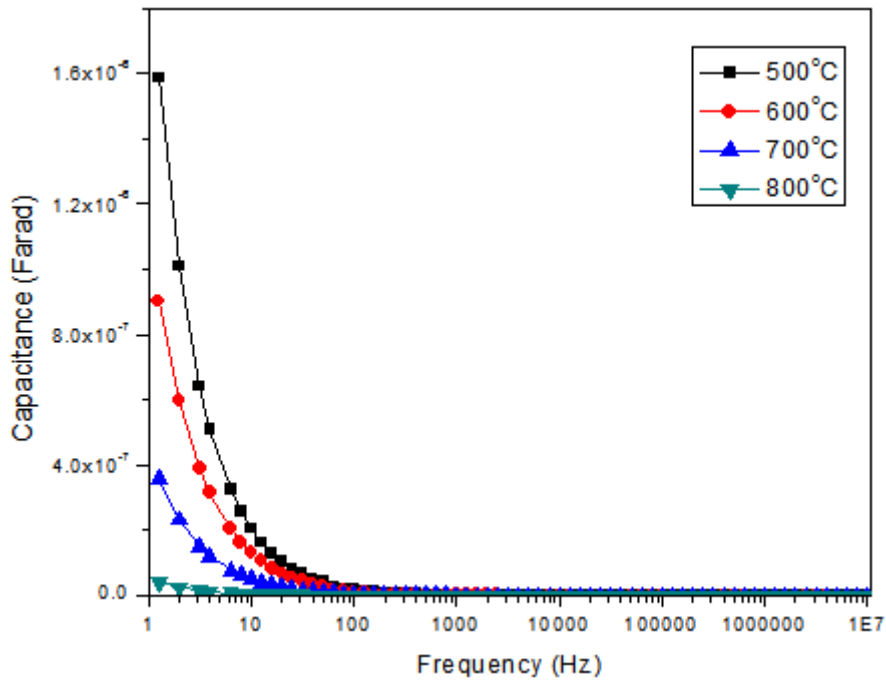


Fig.6: Variation of capacitance with frequency

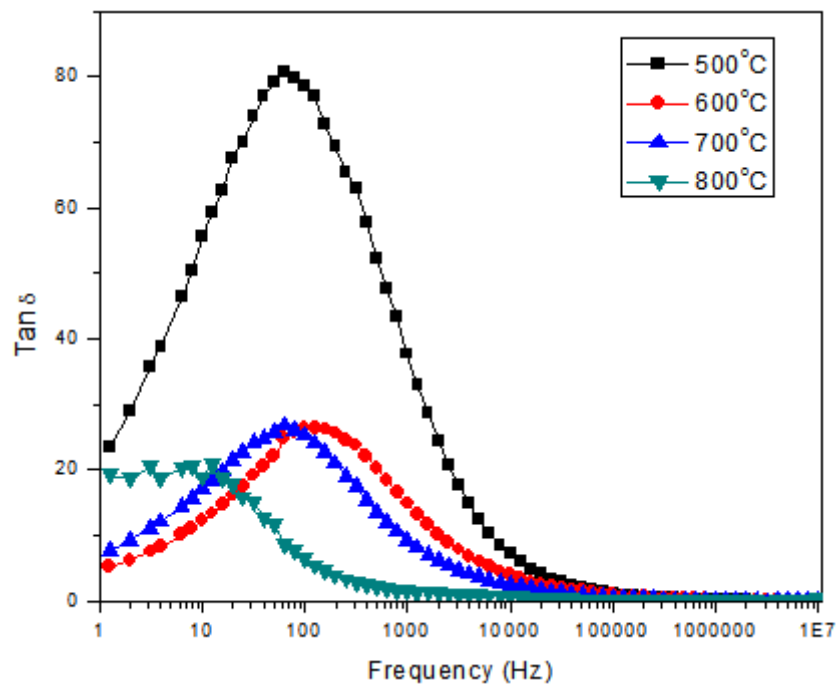


Fig.7: Variation of dielectric loss tangent with frequency

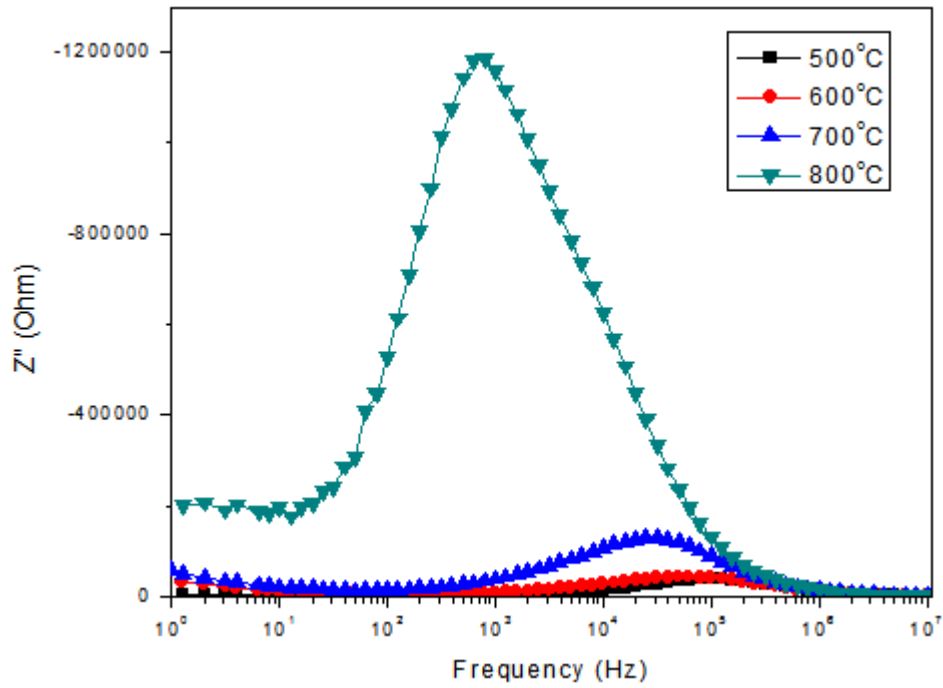


Fig.8: Variation of  $Z''$  with frequency at different temperatures of  $\text{Co}_{0.5}\text{Ti}_{0.5}\text{ZnFeO}_4$

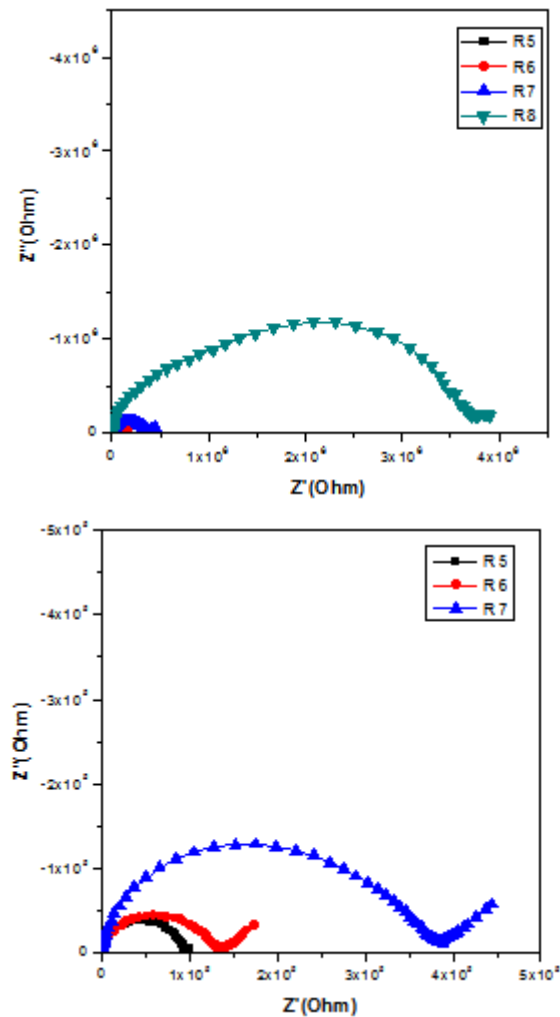


Fig.9: Cole-Cole plots in the frequency range 1 Hz-10 MHz of  $\text{Co}_{0.5}\text{Ti}_{0.5}\text{ZnFeO}_4$